Electromagnetic Detection of Dielectric Cylinders by a Neural Network Approach

Salvatore Caorsi and Paolo Gamba, *Member, IEEE*

***Abstract*—In this paper, the neural network approach is applied to the detection of cylindric objects as well as their geometric and electrical characteristics inside a given investigation domain. The electric field values scattered by the object and available at a small number of locations are fed into the network, whose output is the dielectric permittivity, and the location and radius of the cylinder. The results are evaluated using different sets of testing data, and the dependence of the various output parameters to the input are considered.**

The algorithm performance shows that the approach is able to solve the inverse scattering problem quickly. This may be useful for real-time remote-sensing applications.

***Index Terms*—Buried object detection, inverse problems, neural networks.**

I. Introduction

THIS PAPER presents a neural network approach to the solution of an electromagnetic inverse scattering problem: how to find the geometric and dielectric characteristics of unknown cylindric objects inside a given spatial domain from the knowledge of the scattered electric field. The approach exploits some *a priori* knowledge on the geometry of the problem and the inherent capabilities of neural networks to face nonlinear inverse problems.

In the past, many methods have been proposed to solve the electromagnetic inverse scattering problem, mainly by numerical inversion of the integral scattering equations in the spatial domain (see, for instance, [1]–[5]) for a given frequency of the interrogating source even if some multifrequency approaches are being investigated [6], [7].

In this context, cylindric structures have been studied in conjunction with the buried object detection (in boreholes) [8] since, in this situation, the three-dimensional (3-D) problem simplifies to the characterization of a two-dimensional (2-D) section of the ground. In this research field, often the inverse problem is solved by means of a linearized version of the integral equation representing the scattered electromagnetic field (for instance, equivalent current densities in [9], Born approximation in [10], and an iterative procedure in [11]).

Recently, alternative approaches for nonlinear inverse scattering problems have been introduced that employ minimization techniques, both deterministic [12]–[15] and probabilistic ones (for instance, the Markov random field in [16]).

Manuscript received November 6, 1997; revised June 9, 1998.

The authors are with the Dipartimento di Elettronica, Università di Pavia, I-27100 Pavia, Italy (e-mail: caorsi@ele.unipv.it).

Publisher Item Identifier S 0196-2892(99)00842-6.

However, these methods generally are complex and CPU-intensive: very seldom can they be applied directly to the measurements "on the ground" since they require off-line long computations to be performed. Even if modern computers are now sufficiently powerful to cope with these analyses, the need to extract more and more information from growing amounts of data is still challenging the research community toward simplified and/or faster procedures. This is particularly valid for ground penetrating radar (GPR) applications [17], in which the data collected by means of one or more antennas in a single working day may be huge. In this context, neural networks open interesting solution opportunities, together with an acceptable accuracy of the results.

The use of neural networks is not new in the field of electromagnetic inverse problems. A general introduction to the approach can be found in [18]. However, we must note that neural networks have been applied mainly to electrostatic problems (see, for example, [19]–[21]), the recognition of different types of soils or vegetation from radar backscattering data [22], the analysis of rain data [23] or the retrieval of snow parameters [24] from weather radar measurements, or, again, the classification of targets (airplanes, ground vehicles, etc.) in airborne or satellite radar images [25], [26]. Neural network approaches for geophysical inversion are also available (see the review in [27]), but they are based on particular characteristics of the retrieved electromagnetic signal, well related to the wanted quantities (the surface impedance in [28] and the electromagnetic ellipticity in [29]). Moreover, applications to the detection and classification of buried mines can be found in [30] and [31]. In this last case, the time response to an electromagnetic pulse (suitably transformed) is used to detect an object by means of a first neural network and then the object is recognized as a nylon or wood block by a further classifying neural network. A reduction of the dimensionality of the problem is obtained by a suitable preprocessing transform algorithm.

In our research work, the aim is to reconstruct unknown dielectric objects and their dielectric permittivities inside a given investigation domain. In this paper, our approach handles directly the scattered electric field values for a 2-D investigation domain exploiting the *a priori* knowledge on the circular geometry of the dielectric object possibly inside it.

The paper is organized as follows. The following section outlines the approach to use a neural network for the solution of the electromagnetic inverse scattering problem, stressing the choice of the training samples and of the training algorithm.

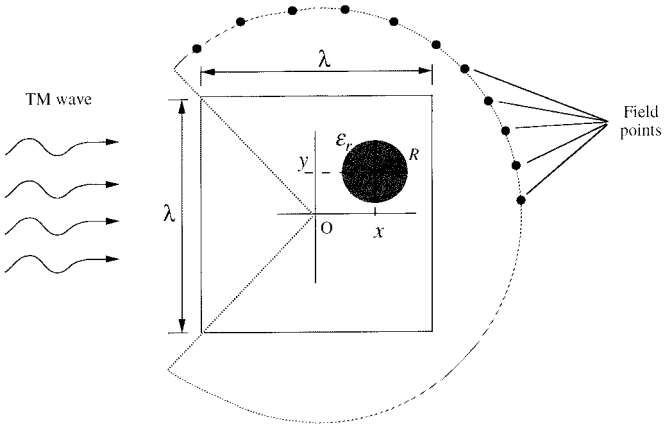

Fig. 1. The physical system under investigation: a circular cylinder with unknown radius r, dielectric permittivity ϵ_r, and center position (x, y) is illuminated by an incident TM wave, and the scattered electric field is measured at some point on a circle centered at the axis origin.

Section III presents the results of the neural reconstruction, first characterizing the network and then discussing the results.

II. Neural Network Inverse Scattering Approach

The problem of the detection and characterization of a dielectric cylinder inside a given investigation domain by means of the scattered field values can be represented in terms of the reconstruction of the dielectric characteristics of a generic body illuminated by an incident electromagnetic wave and by means of the scattered field values available at some points in the space outside the investigation domain. In the following subsections, we will explore the network architecture suitable for the problem and the training data and algorithm.

A. Two-Layer Perceptron

A neural network is a computer model attempting to mimic the behavior of the human brain by combining the capabilities of very simple computing nodes (that correspond to brain neurons). The big advantage of neural networks is that they are completely general tools, and, if suitably tailored to the given problem, they may give faster and similarly exact solutions to the approximation problem than the more traditional methods. The disadvantage is that neural networks must be trained, and this operation (like for the human brain) must be very carefully carried out. Moreover, this step may be very long and CPU-intensive; so, the training sets and the training algorithm play a major role in the neural network approach.

Many different neural networks have been proposed in the literature: the great number of possible architectures allows us to choose the most suitable structure for a given problem. However, as stated in [33], a two-layer feedforward perceptron network with a nonconstant, bounded, and monotone-increasing activation function is sufficient to approximate any nonlinear function $\mathbf{Y} = f(\mathbf{X})$ relating the two sets of variables $\mathbf{X}$ and $\mathbf{Y}$. This is the so-called *universal approximation theorem*.

In our problem, the physical system to be analyzed is presented in Fig. 1, where transverse magnetic (TM) plane waves illuminate a square investigation domain holding eventually a circular cylindric dielectric body with location, radius, and dielectric characteristics that are unknown quantities.

The mathematical formulation of the electromagnetic scattering can be described in its integral form by means of the two well-known electric field integral equations, as follows:

$$\vec{E}(\vec{r}_x) - \vec{E}_{inc}(\vec{r}_x) = \int_D \tau(\vec{r}')\vec{E}(\vec{r}')G(\vec{r}_x/\vec{r}')d\vec{r}' \quad (1)$$

$$\vec{E}_{inc}(\vec{r}') - \vec{E}(\vec{r}') = -\int_D \tau(\vec{r}'')\vec{E}(\vec{r}'')G(\vec{r}'/\vec{r}'')d\vec{r}'' \quad (2)$$

where $\vec{E}_{inc}$ is the incident electric field, $\vec{E}$ is the electric field sum of the incident and the scattered one, D is the given investigation domain, τ is the dielectric permittivity, and $G(u/v)$ is the dyadic Green's function of the particular electromagnetic problem. For instance, if we consider a scatterer in an homogeneous background, $G(u/v)$ is the free-space Green's function, while, if the typical GPR situation is considered (measurement points and scatterer separated by the air-soil interface), $G(u/v)$ represents the half-space Green's function.

With this formulation, the unknown and data quantities $\mathbf{X}$, $\mathbf{Y}$ are, respectively

$$\mathbf{X} = \begin{pmatrix} \tau(\vec{r}) \\ \vec{E}(\vec{r}) \end{pmatrix}, \qquad \text{for } \vec{r} \in D \quad (3)$$

$$\mathbf{Y} = \begin{pmatrix} \vec{E}(\vec{r}_x) - \vec{E}_{inc}(\vec{r}_x) \\ \vec{E}_{inc}(\vec{r}) \end{pmatrix}, \qquad \begin{matrix} \text{for } \vec{r}_x \notin D \\ \text{for } \vec{r} \in D \end{matrix} \quad (4)$$

and the unknown function $f(\cdot)$ corresponds to the system of coupled integrals (1) and (2).

This system defines a very complex nonlinear problem; however, if we exploit the *a priori* information that is in the investigation domain D, only circular cylindric objects can be present. In this way, the unknown variables can be reduced. In particular, they become the coordinates of the location of the section center in the xy plane, its radius, and its dielectric permittivity (magnetic permittivity is considered always equal to one).

In such a case, on behalf of the universal approximation theorem, we can find the unknown dielectric and geometric characteristics of the investigated object by means of a neural network with a single hidden layer, as depicted in Fig. 2. The inputs are the *complex* values of the scattered field, while the outputs are the four unknown variables introduced before.

To complete the discussion about the neural network structure, we need to define the number of necessary inputs, which will be investigated in Section IV, and the number of elements of the hidden layer. Since this latter choice is also difficult to be determined *a priori* [34], we refer to the experimental results section to justify the number of 32 hidden nodes that will be used in the following paragraphs.

B. Training Data Sets

The data sets used for training and testing the network were obtained by a very simple forward model. In fact, for TM plane wave illumination and circular cylinders with known location, radius, and dielectric permittivity (lossless objects

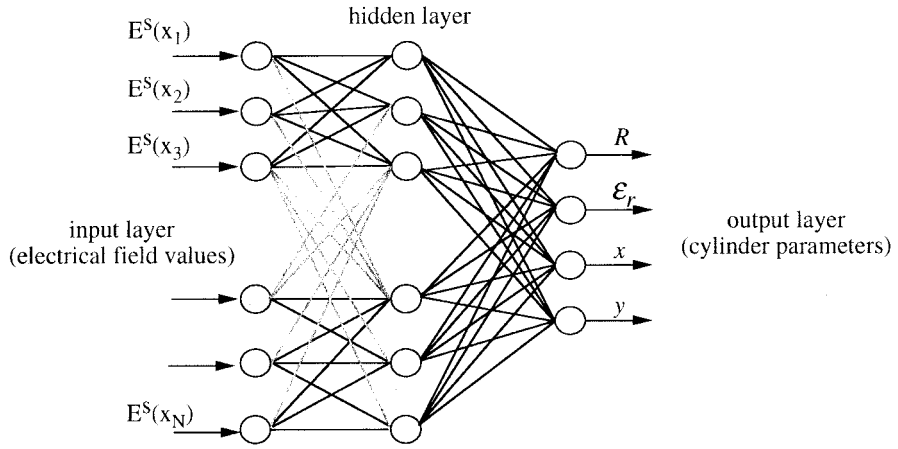

Fig. 2. Neural network structure used for the solution of the electromagnetic inverse scattering problem.

are considered), the scattered electric field can be obtained in a closed form [32]. This model provides the scattered field in a number of points along an arbitrary curve in the xy plane, which, in this case, was chosen as a circular arc centered around the axis origin and opposite to the direction of the incident wave. In particular, 16 equispaced points were chosen along a 3/2 π circular arc (see again Fig. 1).

To train the network, three types of data sets were used, as follows.

- First data set contained scattered field values computed by considering cylindric bodies of known radius and electrical permittivity, arbitrarily located in the xy plane.
- Second data set conversely contained scattered field values computed considering fixed the location but not the electrical and geometric properties of the scatterers.
- Third data set contained scattered field values collected changing arbitrarily all of the parameters characterizing the studied objects.

The reason beyond this choice is that we wanted to test how the different input parameters affect the behavior (convergence and accuracy) of the trained network. This could be of great help in the field since it may define the accuracy that it is required (for training) and obtainable (for detection) in the measurements.

C. Training Algorithm

As mentioned before, the training algorithm is extremely important to obtain meaningful results in a reasonable time, especially when the dimension of the network (like in our choice of the node number) is somehow large.

The usual approach to a two-layer perceptron training is the backpropagation (BP) algorithm [35]. Initially, the weights that define each connection between neurons are randomly chosen. Then, a forward-propagation step computes the output of the network for a given input pattern (the training data). By a comparison of the obtained output with the desired one [usually by a root-mean-square error (rmse)], a suitable indication to update the guessed weight is extracted. In other words, by *backpropagating* the errors by means of a gradient-descent procedure, a correction term to the initial weights can

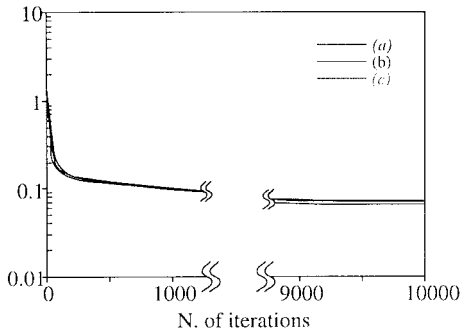

Fig. 3. Absolute error during the training phase for the perceptron network of Fig. 2: (a) the error with a training set of 2500 array of scattered field values and (b) the error with two different training sets of 2000 field values.

be found. By iterating the procedure until convergence, the method moves toward a minimum of the rmse.

However, usually the algorithm is terribly slow and may even fail to lower the rmse. This is due to the critical choice of the learning step in the gradient-descent algorithm (steps that are too big do not converge, ones that are too small converge very slowly) and to the possibility to find a *local* instead of a *global* minimum of the error function.

To solve these problems, a refined version of the BP algorithm, allowing a faster and more precise convergence, was proposed in [36] and adopted in our training step. The so-called *Vogl's acceleration* consists of a more clever choice of the weight updating rule. The learning step is in fact updated at each iteration by means of an acceleration or a deceleration factor. The heuristic under this choice is that, if the error decreases (the direction is correct), the learning step can be safely increased; otherwise, the right direction has been probably lost and a smaller step might be necessary.

We also found it useful that, when dealing with larger dimension's networks, the YPROP algorithm [37] gives a further modification of the BP original procedure by allowing the acceleration and deceleration factors (fixed in the Vogl's acceleration algorithm) to change at each iteration. These factors are chosen to let the learning step increase quickly if it is small, but less quickly when it is already large. In other words, the learning step is no more a linear function of the gradient of the rmse.

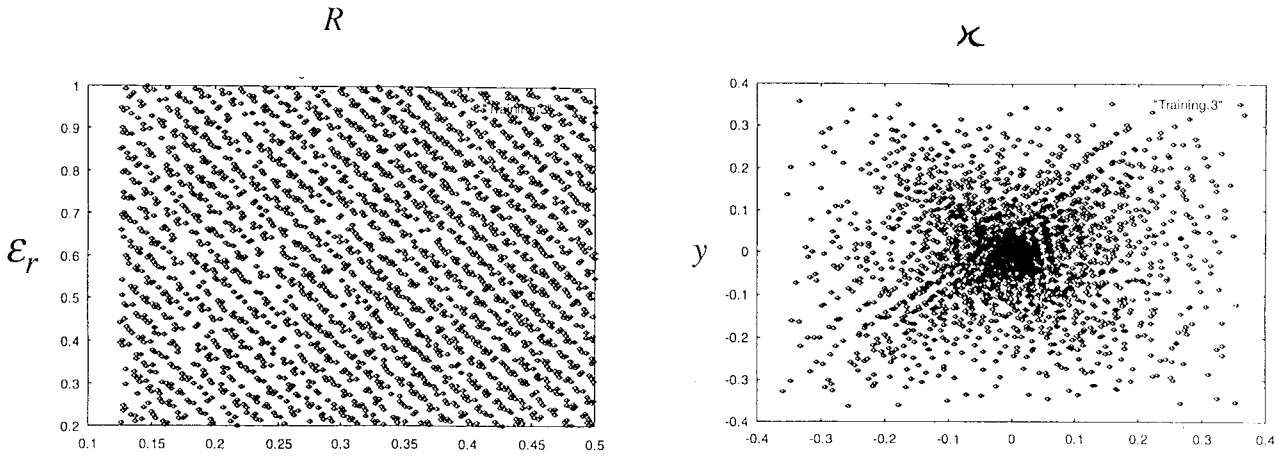

(a) (b)

Fig. 4. Distribution of normalized parameters for a standard training set: (a) R and ϵ_r and (b) the center coordinates x and y.

In Fig. 3, some results showing the convergence of the optimal network as a function of the iteration steps are presented. We observe that, as expected, the use of a larger training set results in a better convergence only as long as the greater number of test points in our four-dimensional (4-D) parameter space means also a better characterization of this same space. Indeed, if the training set is suitably chosen, like in our case, even a relatively small test set is sufficient to assure a reasonably fast convergence for the network's weights.

Fig. 4 represents a typical set of the training arrays used for the preceding processing step, considering on the left the dielectric permittivity ϵ_r and the cylinder radius, and on the right the (x, y) position of the center of the cylinder. All variables are normalized: x, y, and R to λ, ϵ_r to its maximum possible value (taken as five). This set was built by uniformly choosing the first two parameters and randomly considering the position of the cylinder. The only constraint for this choice was that the cylinder section had to be *inside* the investigation domain, a square with side λ. This explains why these latter parameters cluster around the origin.

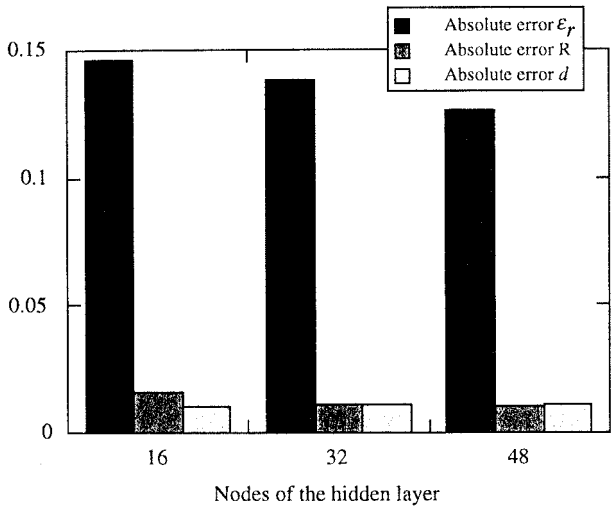

Fig. 5. Mean absolute errors for all normalized output parameters as a function of the number of nodes in the hidden layer.

III. Numerical Experiments

After the training step, the neural network was tested with many, differently taken, data sets obtained again by the forward model. The results are presented in the following paragraphs. We investigate first which of the number of elements in the hidden layer is useful for a good retrieval of the electric and geometric characteristics of the unknown cylindric objects. Then, the stability of the network structure, i.e., the capability to give quite similar weights after training with different training set, is considered. Finally, test results for networks devoted to the retrieval of the dielectric characteristics, or the position, or both, are shown and discussed.

A. Hidden Layer Characterization

It is a very interesting problem to find which is the minimum number of neurons in the hidden layer enabling to obtain satisfying results. To this aim, we considered the possibility of having 16, 32, or 48 neurons in the hidden layer, extracted the weights for the corresponding networks on suitably chosen training sets, and obtained test results. In Fig. 5, we show the mean absolute error for the four output parameters obtained with the different network structures on the same training and test sets. We can see that increasing the number of nodes in the hidden layer leads to a better characterization of the dielectric permittivity and (in a less visible manner) of the cylinder radius. However, the error on $d = \sqrt{x^2 + y^2}$ does not decrease at all. This justifies our choice to use the mean node number (32) in the following analysis steps.

Furthermore, we may observe that mean errors on dielectric permittivity have higher values than corresponding errors on location and radius of the cylinders. This is due to the highest values of ϵ_r (accounting for high permittivity edges in the investigation domain), which give rise to more intense scattered fields and constitute a more difficult situation for the neural network's inversion.

B. Stability Analysis

Another preliminary analysis to assure that the chosen network structure is able to give meaningful results is to consider

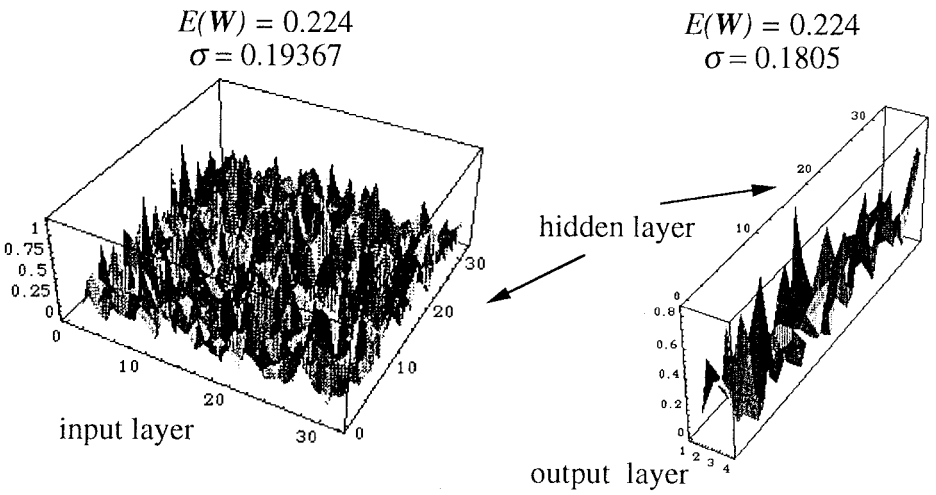

(a) (b)

Fig. 6. Graphical representation of the differences between the elements of the weight matrix ($\mathbf{W}$) for (a) the input-hidden layer interface and (b) the hidden-output layer interface, for a 32-32-4 perceptron network trained with two different training sets. The expected value $E(\mathbf{W})$ and the standard deviation σ of the elements of $\mathbf{W}$ are also shown.

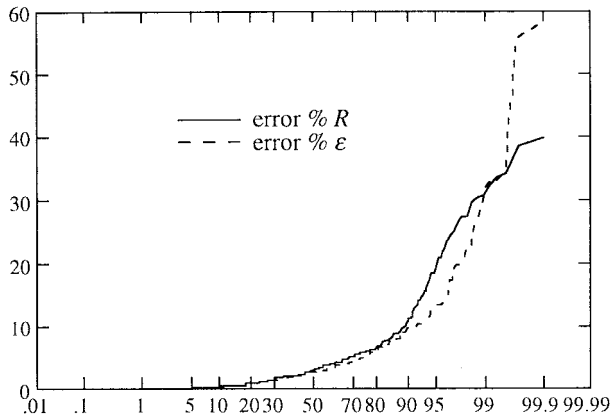

Fig. 7. Cumulative distribution for the percentage errors of a neural network having only R and ϵ_r as output parameters.

what happens when we feed the network with different (but with similar statistics) training sets. To this aim, in Fig. 6(a), the difference (normalized to the maximum weight value) between the elements of the weight matrix $\mathbf{W}$ connecting the input to the hidden layer, obtained in a 32-32-4 network structure after the training with two sets of 2000 arrays, is shown. We observe from the presented mean value $E(\mathbf{W})$ and standard deviation σ that there are generally small differences, even if isolated weights can be extremely different. However, since the network acts globally, these local differences do not affect its behavior in a significant way. The same consideration results from the analysis of the difference between the weight sets connecting the hidden layer to the outputs [Fig. 6(b)].

C. Discussion of the Results

Once the network structure was chosen, we trained and tested the network to find how it can be useful for the electromagnetic inverse scattering problem. First of all, in Fig. 7, the cumulative distributions for the test set errors of a network having only two outputs, the dielectric permittivity ϵ_r and the cylinder radius R, are shown. The graph allows us to observe that more than 90% of the percentage errors have a value smaller than 10%. However, very large percentage errors are still possible. To understand the reason, we present in Tables I and II the absolute errors for ϵ_r and R, after the subdivision of their definition interval into a significant number of parts. We observe that smaller values of R correspond to small absolute errors, which unfortunately give very high percentage errors, contributing to the phenomenon shown in Fig. 7.

Moreover, Table II shows that errors on the dielectric permittivity are concentrated in the higher intervals. This is probably because of the fact that the network acts very similarly with respect to both parameters.

TABLE I
ABSOLUTE ERRORS FOR THE CYLINDER NORMALIZED DIELECTRIC PERMITTIVITY ϵ_r FOR A NETWORK HAVING ONLY R AND ϵ_r AS OUTPUT PARAMETERS

Normalize ϵ_r range	Absolute mean error	Standard Deviation
$0.20 \leq \epsilon_r < 0.36$	0.039323	0.043017
$0.36 \leq \epsilon_r < 0.52$	0.044993	0.045829
$0.52 \leq \epsilon_r < 0.68$	0.045746	0.043235
$0.68 \leq \epsilon_r < 0.84$	0.058604	0.042017
$0.84 \leq \epsilon_r \leq 1.00$	0.102166	0.081737

TABLE II
ABSOLUTE ERRORS FOR THE CYLINDER NORMALIZED RADIUS R FOR A NETWORK HAVING ONLY R AND ϵ_r AS OUTPUT PARAMETERS

Normalized R range	Absolute mean error	Standard Deviation
$0.125 \leq R < 0.200$	0.033718	0.031853
$0.200 \leq R < 0.275$	0.023228	0.022905
$0.275 \leq R < 0.350$	0.024579	0.018878
$0.350 \leq R < 0.425$	0.024685	0.024889
$0.425 \leq R \leq 0.500$	0.020142	0.016699

TABLE III
ABSOLUTE ERRORS FOR THE CYLINDER CENTER NORMALIZED COORDINATES x AND y FOR A NETWORK HAVING ONLY THESE PARAMETERS AS OUTPUTS

Normalized x range	Normalized y range	Absolute mean error	Standard Deviation
-0.3750 $\leq x <$ -0.1875	-0.3750 $\leq y <$ -0.1875	0.090282	0.066952
-0.3750 $\leq x <$ -0.1875	-0.1875 $\leq y <$ 0.0000	0.060318	0.064339
-0.3750 $\leq x <$ -0.1875	0.0000 $\leq y <$ 0.1875	0.044763	0.028740
-0.3750 $\leq x <$ -0.1875	0.1875 $\leq y \leq$ 0.3750	0.081964	0.032396
-0.1875 $\leq x <$ 0.0000	-0.3750 $\leq y <$ -0.1875	0.051833	0.019309
-0.1875 $\leq x <$ 0.0000	-0.1875 $\leq y <$ 0.0000	0.033596	0.023256
-0.1875 $\leq x <$ 0.0000	0.0000 $\leq y <$ 0.1875	0.030475	0.023685
-0.1875 $\leq x <$ 0.0000	0.1875 $\leq y \leq$ 0.3750	0.073926	0.046449
0.0000 $\leq x <$ 0.1875	-0.3750 $\leq y <$ -0.1875	0.066680	0.037817
0.0000 $\leq x <$ 0.1875	-0.1875 $\leq y <$ 0.0000	0.032035	0.018585
0.0000 $\leq x <$ 0.1875	0.0000 $\leq y <$ 0.1875	0.032267	0.023839
0.0000 $\leq x <$ 0.1875	0.1875 $\leq y \leq$ 0.3750	0.062130	0.048264
0.1875 $\leq x \leq$ 0.3750	-0.3750 $\leq y <$ -0.1875	0.111975	0.038690
0.1875 $\leq x \leq$ 0.3750	-0.1875 $\leq y <$ 0.0000	0.042045	0.026925
0.1875 $\leq x \leq$ 0.3750	0.0000 $\leq y <$ 0.1875	0.055227	0.076007
0.1875 $\leq x \leq$ 0.3750	0.1875 $\leq y \leq$ 0.3750	0.082520	0.069905

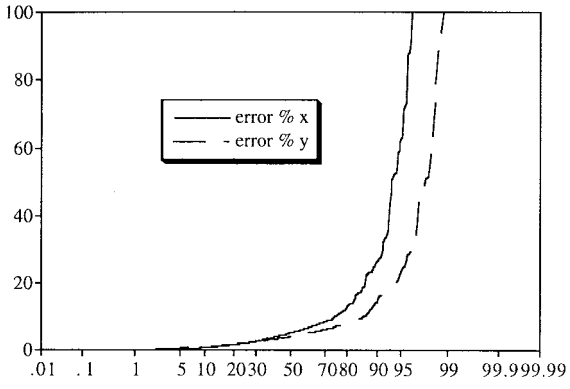

Fig. 8. Cumulative distribution for the percentage errors of a neural network having only x and y as output parameters.

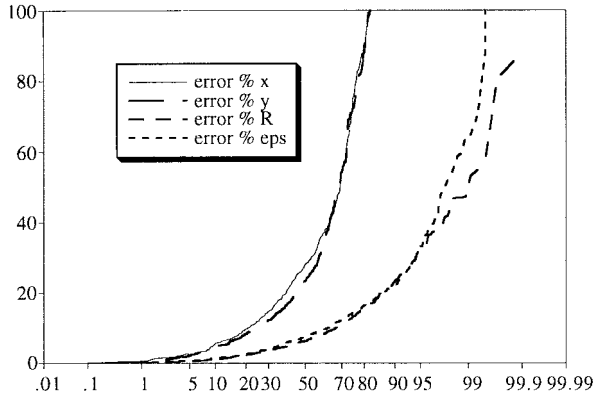

Fig. 9. Cumulative distribution for the percentage errors of a neural network having all four outputs R, ϵ_r, x, and y.

To study the capabilities of the neural inversion to detect the position of a cylinder of given radius and dielectric permittivity, a second network was trained. Similarly to the previous paragraphs, we present in Fig. 8 the cumulative distributions of the percentage errors, showing a worse behavior than the preceding parameters. However, a look to Table III confirms that the reason is the same as for R. Since here both x and y belong to $[-3/8\lambda, 3/8\lambda]$, their distribution, as highlighted by Fig. 4, is clustered around the origin. Therefore, very high percentage errors correspond to very small values of the (x, y) pair.

Finally, Fig. 9 refers to a complete neural network with four outputs, 32 inputs, and 32 nodes in the hidden layer. Its behavior is very similar, for the two parameters pairs, to the ones of the partial networks presented before, showing that the geometric and dielectric characteristics of the unknown circular cylinder are practically independent, or at least uncorrelated. Despite the cumulative distributions, the networks behave well when globally considered. Fig. 10 graphically represents the mean position of an unknown cylinder together with its mean radius, as obtained in a test set by the neural network (dashed line), compared with the same quantities for the actual test set. Undoubtfully, there is a strong similarity, especially if we consider that the difference between the mean ϵ_r values are not shown because it is invisible, even using a 256-tone grayscale.

IV. CONCLUSIONS

In this work, we have presented the application of a neural network approach to the electromagnetic inverse scattering problem. We have shown that a suitable network could be able to give a sufficiently accurate solution to the problem of retrieving the position, radius, and dielectric permittivity of an

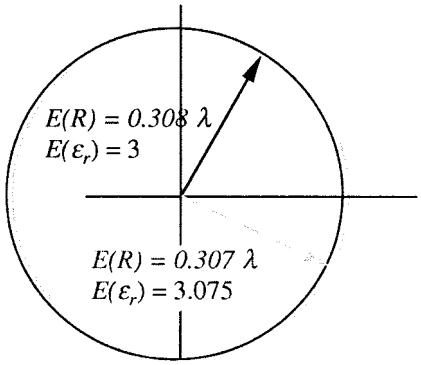

Fig. 10. Graphical representation of the mean position of an unknown cylinder together with its mean radius, as obtained in a test set by the neural network (in light grey), compared with the same quantities for the actual test set.

unknown circular cylinder illuminated by a TM wave, starting from the knowledge of the scattered electric field.

The stability and accuracy of the results has been investigated, with particular stress on the possibility to build specialized networks devoted to the separate extraction of the dielectric and geometric characteristics of the scatterer.

The results are encouraging, and they show that the application of a neural approach to the electromagnetic inverse scattering is valid and that more research should be done to widen this extremely interesting method to more general situations. Eventually, we hope to come to the recognition, from the scattered electric field, of the dielectric permittivity in any point inside a given investigation domain, and this is the direction of our current study in the field.

REFERENCES

[1] J. C. Bolomey, "Recent European developments in active microwave imaging for industrial, scientific, and medical applications," *IEEE Trans. Microwave Theory Tech.*, vol. 37, pp. 2109–2117, Nov. 1989.

[2] S. Caorsi, G. L. Gragnani, and M. Pastorino, "Two-dimensional microwave imaging by a numerical inverse scattering solution," *IEEE Trans. Microwave Theory Tech.*, vol. 38, pp. 981–989, Aug. 1990.

[3] N. Joachimwicz, C. Pichot, and J. P. Hugonin, "Inverse scattering: An iterative numerical method for electromagnetic imaging," *IEEE Trans. Antennas Propagat.*, vol. 39, pp. 1742–1752, Dec. 1991.

[4] S. Caorsi, G. L. Gragnani, and M. Pastorino, "Redundant electromagnetic data for microwave imaging of three-dimensional dielectric objects," *IEEE Trans. Antennas Propagat.*, vol. 42, pp. 581–658, May 1994.

[5] C. Pichot, "Spectral and spatial-domain techniques for microwave imaging," in *Proc. Workshop Inverse Scattering Microw. Imaging, 25th Eur. Microw. Conf.*, Bologna, Italy, Sept. 1995, pp. 85–90.

[6] S. Caorsi, G. L. Gragnani, and M. Pastorino, "Stochastic modeling of multifrequency inverse scattering by inhomogeneous dielectric objects," in *Proc. 195 URSI Symp. Electromagn. Theory*, St. Petersburg, Russia, May 23–26, 1995, pp. 267–269.

[7] K. Belkebir, R. E. Kleinmann, and C. Pichot, "Microwave imaging location and shape reconstruction from multifrequency scattering data," *IEEE Trans. Microwave Theory Tech.*, vol. 45, pp. 469–476, Apr. 1997.

[8] G. A. Ellis and I. C. Peden, "An analysis technique for buried inhomogeneous dielectric objects in the presence of an air-earth interface," *IEEE Trans. Geosci. Remote Sensing*, vol. 33, pp. 535–540, May 1995.

[9] S. Caorsi, G. L. Gragnani, and M. Pastorino, "Numerical electromagnetic inverse-scattering solutions for two-dimensional infinite dielectric cylinders buried in a lossy half-space," *IEEE Trans. Microwave Theory Tech.*, vol. 41, pp. 352–356, Feb. 1993.

[10] E. L. Miller and A. S. Willsky, "A multiscale, statistically based inversion scheme for linearized inverse scattering problems," *IEEE Trans. Geosci. Remote Sensing*, vol. 34, pp. 346–357, Mar. 1996.

[11] P. Chaturvedi and R. G. Plumb, "Electromagnetic imaging of underground targets using constrained optimization," *IEEE Trans. Geosci. Remote Sensing*, vol. 33, pp. 551–561, May 1995.

[12] R. E. Kleinman and P. M. van den Berg, "Two-dimensional location and shape reconstruction," *Radio Sci.*, vol. 29, p. 1157, 1994.

[13] J. J. Mallorquì and A. Broquetas, "Microwave inverse scattering: Biomedical and industrial applications," in *Proc. Progress Electromagn. Res. Symp.*, Seattle, WA, 1995.

[14] S. Caorsi, S. Ciaramella, G. L. Gragnani, and M. Pastorino, "On the use of regularization techniques in numerical inverse scattering solutions for microwave imaging applications," *IEEE Trans. Microwave Theory Tech.*, vol. 43, pp. 632–640, May 1995.

[15] P. Lobel, C. Pichot, L. Blancferrand, and M. Barlaud, "A new regularization scheme for inverse scattering inverse problems," *Inv. Probl.*, vol. 13, pp. 403–410, Apr. 1997.

[16] S. Caorsi, G. L. Gragnani, S. Medicina, M. Pastorino, and G. A. Pinto, "A Gibbs random field based active electromagnetic method for noninvasive diagnostics in biomedical applications," *Radio Sci.*, vol. 30, pp. 291–301, 1995.

[17] L. Peters, Jr., J. J. Daniels, and J. D. Young, "Ground penetrating radar as a subsurface environmental sensing tool," *Proc. IEEE*, vol. 82, pp. 1802–1822, Dec. 199?.

[18] I. Elshafiey, L. Udpa, and S. S. Udpa, "Solution of inverse problems in electromagnetics using Hopfield neural networks," *IEEE Trans. Magn.*, vol. 31, pp. 852–861, Jan. 1995.

[19] T. S. Low and B. Chao, "The use of finite elements and neural networks for the solution of inverse electromagnetic problems," *IEEE Trans. Magn.*, vol. 28, pp. 2811–2813, Sept. 1992.

[20] S. R. H. Hoole, "Artificial neural networks in the solution of inverse electromagnetic field problems," *IEEE Trans. Magn.*, vol. 29, no. 2, pp. 1931–1934, Mar. 1993.

[21] I. T. Rekanos and T. D. Tsiboukis, "Electromagnetic filed inversion using the quickprop method," *IEEE Trans. Magn.*, vol. 33, pp. 1872–1875, Mar. 1997.

[22] M. S. Dawson, A. K. Fung, and M. T. Manry, "A robust statistical-based estimator for soil moisture retrieval from radar measurements," *IEEE Trans. Geosci. Remote Sensing*, vol. 35, pp. 57–67, Jan. 1997.

[23] R. Xiao and V. Chandrasekar, "Development of a neural network based algorithm for rainfall estimation from radar observation," *IEEE Trans. Geosci. Remote Sensing*, vol. 35, pp. 160–171, Jan. 1997.

[24] D. T. Davis, Z. Chen, L. Tsang, J. N. Hwang, and A. T. C. Chang, "Retrieval of snow parameters by iterative inversion of a neural network," *IEEE Trans. Geosci. Remote Sensing*, vol. 31, pp. 842–852, July 1993.

[25] M. V. Shirvaikar and M. M. Trivedi, "A neural network filter to detect small targets in high clutter backgrounds," *IEEE Trans. Neural Networks*, vol. 6, pp. 252–257, Jan. 1995.

[26] S. Chkrabarti, N. Bindal, and K. Theagharajan, "Robust target classifier using artificial neural networks," *IEEE Trans. Neural Networks*, vol. 6, pp. 760–766, May 1995.

[27] A. Raiche, "A pattern recognition approach to geophysical inversion using neural networks," *Geophys. J. Int.*, vol. 105, pp. 629–648, 1991.

[28] H. Hidalgo and E. Gomez-Trevino, "Application of constructive learning algorithms to the inverse problem," *IEEE Trans. Geosci. Remote Sensing*, vol. 34, pp. 874–885, July 1996.

[29] M. Poulton, E. K. Sternberg, and C. E. Glass, "Neural network patterns recognition of subsurface images," *J. Appl. Geophys.*, vol. 29, pp. 21–36, 1992.

[30] M. R. Azimi-Sadjandi, D. E. Pole, S. Sheedvash, K. D. Sherbondy, and S. A. Stricker, "Detection and classification of buried dielectric anomalies using a separated aperture sensor and a neural network discriminator," *IEEE Trans. Instrum. Meas.*, vol. 41, pp. 137–143, Feb. 1992.

[31] M. R. Azimi-Sadjandi and S. A. Stricker, "Detection and classification of buried dielectric anomalies using neural networks—Further results," *IEEE Trans. Instrum. Meas.*, vol. 43, pp. 34–39, Feb. 1994.

[32] D. S. Jones, *The Theory of Electromagnetism.* New York: Pergamon, 1964.

[33] S. Haykin, *Neural Networks.* New York: Macmillan, 1994.

[34] H. Bischof, W. Schneider, and A. J. Pinz, "Multispectral classification of Landsat images using neural networks," *IEEE Trans. Geosci. Remote Sensing*, vol. 30, pp. 482–490, Mar. 1992.

[35] D. E. Rumelhart, G. E. Hinton, and R. H. Williams, "Learning representations by backpropagating errors," *Nature*, vol. 323, pp. 533–536, 1986.

[36] T. P. Vogl, J. K. Mangis, A. K. Rigler, W. T. Zink, and D. L. Alkon, "Accelerating the convergence of the back-propagation method," *Biol. Cybern.*, vol. 59, pp. 257–263.

[37] D. Anguita, M. Pampolini, G. Parodi, and R. Zunino, "YPROP: Yet another accelerating technique for the back propagation," in *Proc. Int. Conf. Artif. Neural Networks*, Amsterdam, The Netherlands, Sept. 13–16, 1993, pp. 500–503.

Salvatore Caorsi received the laurea degree in electronic engineering from the University of Genoa, Genoa, Italy, in 1973.

He was with the University of Genoa as a Researcher, and since 1976, he has been an Associate Professor of antennas and propagation in the Department of Biophysical and Electronic Engineering, University of Genoa. In 1985, he also assumed the title of Professor of fundamentals of remote sensing. Since 1994, he has been a Full Professor of electromagnetic compatibility, Department of Electronics, University of Pavia, Pavia, Italy. His primary activities focus on applications of electromagnetic fields to telecommunications, artificial vision and remote sensing, biology, and medicine. In particular, he is working on research projects concerning human hazard to electromagnetic exposure, numerical methods for solving electromagnetic problems, wave interaction in the presence of nonlinear media, inverse scattering and microwave imaging, and electromagnetic compatibility.

Dr. Caorsi is the past President and funding member of the Inter-University Research Center for Interactions between Electromagnetic Fields and Biological Systems (ICEmB). He is a member of the Associazione Elettrotecnica Italiana (AEI), the European Bioelectromagnetism Association (EBEA), and the European Society for Hyperthermic Oncology (ESHO).

Paolo Gamba (S'91–M'93) was born in Cremona, Italy, on April 5, 1965. He received the laurea degree in electronic engineering (cum laude) in 1989 and the Ph.D. degree in electromagnetics in 1993 from the University of Pavia, Pavia, Italy.

He was an R&D Engineer in the Microwave Laboratory, Siemens Telecomunicazioni, Cassina de' Pecchi, Milano, Italy, from 1992 to 1994. In 1994, he joined the Department of Electronics, University of Pavia, first as a Teaching Assistant and now as an Assistant Professor. Since 1997, he has been teaching radio communications systems. His current research interests include efficient methods for the inverse scattering of GPR measurements, synthetic array radar data analysis (especially over urban areas), and meteorological radar processing.